

Earth's Future



RESEARCH ARTICLE

10.1029/2024EF004697

Key Points:

- We conducted the first global analysis of soil moisture effects on population exposure to heatwaves
- Effects of projected soil moisture changes constitute a strong component in the exacerbation of heatwaves over most land regions
- Population exposure to heatwaves rises sharply in Asia, Australia, US, Europe, and central and southern Africa

Supporting Information:

Supporting Information may be found in the online version of this article.

Correspondence to:

J. Zhou and A. L. Hirsch, jingwei.zhou@wur.nl; annette.l.hirsch@gmail.com

Citation:

Zhou, J., Teuling, A. J., Seneviratne, S. I., & Hirsch, A. L. (2024). Soil moisture-temperature coupling increases population exposure to future heatwaves. *Earth's Future*, 12, e2024EF004697. https://doi.org/10.1029/2024EF004697

Received 19 MAR 2024 Accepted 13 MAY 2024

Author Contributions:

Conceptualization: Jingwei Zhou,

Annette L. Hirsch

Formal analysis: Jingwei Zhou, Adriaan J. Teuling, Sonia I. Seneviratne, Annette I. Hirsch

Methodology: Jingwei Zhou, Annette

L. Hirsch

Project administration: Jingwei Zhou,

Adriaan J. Teuling

Software: Jingwei Zhou, Annette

L. HIISCH

Supervision: Adriaan J. Teuling, Annette

L. Hirsch

Validation: Jingwei Zhou Visualization: Jingwei Zhou

Writing – original draft: Jingwei Zhou Writing – review & editing: Jingwei Zhou, Adriaan J. Teuling, Sonia

Jingwei Zhou, Adriaan J. Teuling, Sor I. Seneviratne, Annette L. Hirsch

© 2024. The Author(s).

This is an open access article under the terms of the Creative Commons
Attribution License, which permits use, distribution and reproduction in any medium, provided the original work is properly cited.

Soil Moisture-Temperature Coupling Increases Population Exposure to Future Heatwaves

Jingwei Zhou^{1,2}, Adriaan J. Teuling¹, Sonia I. Seneviratne³, and Annette L. Hirsch^{4,5}

¹Hydrology and Environmental Hydraulics Group, Wageningen University & Research, Wageningen, The Netherlands, ²Research School of Earth Sciences, The Australian National University, Canberra, ACT, Australia, ³Institute for Atmospheric and Climate Science, ETH Zurich, Zürich, Switzerland, ⁴ARC Centre of Excellence for Climate Extremes, The University of New South Wales, Sydney, NSW, Australia, ⁵Climate Change Research Centre, The University of New South Wales, Sydney, NSW, Australia

Abstract Heatwaves have significant effects on ecosystems and human health. Human habitability is impacted severely as human exposure to heatwaves is projected to increase, however, the contribution of soil moisture effects to the increased exposure is unknown. We use data from four climate models, in which two experiments are used to isolate soil moisture effects and in this way to examine projected changes of soil moisture contributions to projected increases in heatwave events. Contributions from soil moisture to future population exposure to heatwaves are also investigated. With soil moisture effects combined with global warming, the longest yearly heatwaves are found to increase by up to 20 days, intensify by up to 2°C in mean temperature, with an increasing of frequency by 15% (the percentage relative to the total number of days for a year) over most mid-latitude land regions by 2040–2070 under the SSP585 high emissions scenario. Furthermore, soil moisture changes are found to have a significant role in projected increases of multiple heatwave characteristics regionally compared with the global land area and contribute to more global population exposed to heatwaves.

Plain Language Summary Heatwaves have great impacts on human health, agriculture, economy, and many other related societal factors. Existing research has not formed a comprehensive understanding of the influences from soil moisture and drought on population exposure to global heatwaves. This study aims to provide a better perception and quantification of soil moisture effects on changes of both heatwaves per se and population exposure to heatwaves, which will help to enhance further insights of climate change impacts on human society. Using outputs from dedicated climate model experiments, it is found detectable contributions from soil moisture changes on exacerbating heatwaves and increasing population exposure to them. This study can inform evidence-based policies and potential land management techniques such as irrigation, land radiative management, and forestation, for mitigating the impacts of climate extremes.

1. Introduction

Recent decades have seen an increasing trend in heatwave duration, frequency, and intensity worldwide (Cowan et al., 2014; Miralles et al., 2014; Perkins-Kirkpatrick & Lewis, 2020; Perkins et al., 2012; Seneviratne et al., 2021). In the 2020 Northern Hemisphere summer, across the south-western and north-eastern US, eastern Canada, and northern Russia, the seasonal temperature was at least 2.0°C above average ("State of the Climate: Global Climate Report for August 2020," 2020). In 2022, extreme heat events continued throughout India and Pakistan, where the temperature in Pakistan recorded 49°C (Zachariah et al., 2023). For the Southern Hemisphere, the summer from December 2019 to February 2020 was the hottest on record for Australia. During December 2019, 11 days, in which the national area-averaged maximum was 40°C or above, were among this unusually extended period of heatwave over much of Australia. In the context of global land, the year 2020 ranked the warmest year in the 141-year record and had an average land temperature of +1.59 K above pre-industrial levels ("State of the Climate: Global Climate Report for Annual, 2020," 2020).

Effects of soil moisture in amplifying hot temperature extremes in past and present climate have been widely explored in recent decades (Dirmeyer et al., 2021; Lorenz et al., 2016; Seneviratne et al., 2010, 2013; Zhang et al., 2011). Most previous studies on soil moisture-temperature (hereafter S-T) coupling during heatwaves had a regional focus (Fischer et al., 2007; Geirinhas et al., 2022; Hauser et al., 2016; Lewis & King, 2015; Vogel et al., 2018; Zhang et al., 2011). So far, research comparing the mechanisms of heatwaves across regions using a

ZHOU ET AL. 1 of 13

consistent methodology is more limited (Lorenz et al., 2016). As the spatial heterogeneity of land surface conditions (e.g., vegetation, soil moisture, and land use), precipitation variability, and atmospheric dynamics contributes to regional differences in S-T interactions and heatwaves (A. L. Hirsch & King, 2020; A. L. Hirsch et al., 2019; Seneviratne et al., 2010; Teuling et al., 2010; S. Zhou & Yuan, 2022), the quantification and distinction of how much regional land surface contributions to heatwaves vary globally, is of primary importance. In particular, it is necessary to avoid generalizing land surface contributions when it has been demonstrated that effects of projected soil moisture changes on heat extremes vary spatially (Seneviratne et al., 2010) and land feedbacks are teleconnected in propagating heat extremes (Miralles et al., 2019; S. Zhou & Yuan, 2022). As great decreases of summer soil moisture and water limitation are widely found across the world (Denissen et al., 2022; McKinnon et al., 2021) and the impacts from heatwaves are projected to increase under future warming (Miralles et al., 2019; Perkins-Kirkpatrick & Lewis, 2020; Perkins et al., 2012; Seneviratne et al., 2006, 2021), investigating future changes in soil moisture effects on hot temperature extremes could help to better understand regional differences in projected heatwave characteristics. Different management strategies are required to cope with shorter and more intense heatwaves or longer and less intense heatwaves (Perkins-Kirkpatrick & Lewis, 2020). Investigations on different heatwave characteristics can facilitate more appropriate combinations of future community adaption methods and mitigation policies against heatwave impacts.

Existing research is often focused on the population exposure to heatwaves per se and its influences on the mortality and morbidity of people (Jones et al., 2018; Mishra et al., 2017). Yang et al. (2021) found that heat-related excess mortality is projected to increase from 1.9% in the 2010s to 5.5% (0.5%–9.9%) in the 2090s under Representative Concentration Pathway 8.5 (RCP8.5) in China (Yang et al., 2021). With different heatwave definitions used, heatwave-related mortality risks increased by a range of 3%–16% globally (Xu et al., 2016). However, population exposure to heatwaves is rarely investigated from a soil moisture perspective, despite its relevance to temperatures on timescales ranging from heatwave events to long-term temperature trends. As soil moisture effects tend to amplify heatwaves (Miralles et al., 2014; Qiao et al., 2023) and more severe heatwaves lead to higher population exposure to heat stress and related health risks (Jones et al., 2018; Mora et al., 2017), which highlights the importance of considering soil moisture when assessing heatwave risks for human populations. In this study we investigate the contribution of soil moisture changes, that is, the soil moisture variability and trend beyond its climatological value of the recent historical climate as induced both by S-T interactions and climate change, to increases of heatwave characteristics and how this relates to future changes in population exposure to extreme heat.

2. Methods

2.1. Heatwave Identification and Classification

Many different methods and indices exist to characterize heatwave (Perkins, 2015; Perkins & Alexander, 2013). Here, we use a modified excess heat factor (EHF) to define such events where at least three consecutive days are above a threshold temperature (Cowan et al., 2014; Perkins et al., 2015). Numerous national meteorological agencies such as the Australian Bureau of Meteorology, Met Office in UK, and National Oceanic and Atmospheric Administration (NOAA) have used or are considering using the excess heat factor (EHF) to identify heatwave days and describe important characteristics of heatwaves (Hudson & Marshall, 2016; J. Nairn et al., 2018). A modified version of EHF is used in this study to identify heatwave days (J. R. Nairn & Fawcett, 2014; Perkins & Alexander, 2013). This index can be expressed as:

$$EHF_{sig} = T_{3d} - T_{90} = \frac{(T_i + T_{i+1} + T_{i+2})}{3} - T_{90}$$
 (1)

where T_i is the average daily temperature for day i, and T_{90} is the calendar day 90th percentile of daily average temperature using all the reference years investigated (1980–2014). The World Meteorological Organization defines a heatwave day (HWD) using a reference period of 1961–1990. However, due to the ongoing temperature increases globally, our approaches of using a relatively recent reference period are likely to identify slightly fewer heatwave days but indicate a more relevant heatwave projection in respect to a more recent reference. The average daily temperature is defined as the average of T_{\min} (i.e., daily minimum temperature) and T_{\max} (i.e., daily maximum temperature) within a 24-hr cycle. Use of this definition facilitate the effects from both T_{\min} and T_{\max} , as high T_{\min} has been shown to have particular health impacts (Thorne et al., 2016).

ZHOU ET AL. 2 of 13



Earth's Future

10.1029/2024EF004697

Table 1
Climate Models Participating in CMIP6 That Are Used in This Research

		Resolution	
Name	Institute	(km)	References
EC-Earth	Swedish Meteorological and Hydrological Institute (SMHI) and 30 other institutes	100	Döscher et al. (2022)
IPSL- CM6	Institut Pierre Simon Laplace (IPSL)	250	Boucher et al. (2020) and Lurton et al. (2020)
MIROC6	Japan Agency for Marine-Earth Science and Technology (JAMSTEC) Atmosphere and Ocean Research Institute (AORI) National Institute for Environmental Studies (NIES)	250	Tatebe et al. (2019)
MPI-ESM	Max Planck Institute for Meteorology (MPI-M)	250	Mauritsen et al. (2019)
			<u> </u>

Note. Please refer to Eyring et al. (2016), O'Neill et al. (2016), Tebaldi et al. (2021), and van den Hurk et al. (2016) for more details.

 T_{90} is estimated using a 15-day window (i.e., 7 days before and after the calendar day with a temperature T_t) for all reference years to provide a sample of 525 (15 × 35) daily values per grid cell. Positive values of EHF_{sig} define heatwave-like conditions for day t. If the T_{3d} is above the threshold of T_{90} for at least three consecutive days (i.e., EHF_{sig} , EHF_{sig} , EHF_{sig} , and EHF_{sig} are all above 0), these days are regarded as heatwave days.

With heatwave days identified, different heatwave characteristics have been calculated on a yearly basis. In this study, different characteristics of heatwaves such as duration of the seasonal longest heatwave (HWD); average magnitude for all seasonal heatwaves (HWMt); temperature at the peak of the heatwave with the hottest average (HWAt); number of heatwave days (HWF), which is expressed as the percentage relative to the total number of days, are analyzed.

The heatwaves during the summer-centering period are the focus of our research. The summer-centering period in the Northern Hemisphere is defined as May, June, July, August, and September; the summer-centering period in the Southern Hemisphere is defined as November, December, January, February, and March. Moreover, January, February, and March of the next year are moved forward to the year before to calculate summer heatwave characteristics of a specific year in the Southern Hemisphere.

2.2. Detection of Soil Moisture Impacts on Heatwaves

Each of the four climate models (please refer to Table 1 for more information regarding the climate models we used) within Coupled Model Intercomparison Project phase 6 (CMIP6), used in this research performs a fully coupled control run (CTL), and two experiments (pdLC and rmLC) where soil moisture is prescribed. In this paper, only one of the experiments (pdLC) is used with CTL to quantify effects of soil moisture changes in the form of CTL-pdLC. Soil moisture in pdLC is prescribed by the 1980–2014 climatological values calculated from the control simulation (please refer to Section 3.1 for more information regarding the experiments within the CMIP6 data set). To understand contributions of soil moisture changes to each of the heatwave characteristics, estimates of comparison (CTL and pdLC) for each heatwave characteristic are investigated (Figure 1).

Statistical significance in comparisons of heatwave characteristics between present period (2000–2030) and future period (2040–2070) (Figures S4 and S5 in Supporting Information S1) and between CTL and pdLC (show how strong the soil moisture contributions are; Figure 1 and Figure S1 in Supporting Information S1) are assessed using a Kolmogorov-Smirnov test (KS test) (Hodges, 1958). Comparisons between a current period of 2000–2030 and a closer future period of 2040–2070 rather than ones between a historical period and a further period such as 2070–2100 guarantee a more relevant investigation on the changes in heatwave characteristics and population exposure to those heatwave characteristics.

To determine the total contributions of S-T coupling to the changes in temperature extremes at regional scales, projected changes in heatwave characteristics and population exposure to these characteristics are computed, the differences of the changes between CTL and pdLC express the role of soil moisture to changes in heatwave characteristics and population exposure to those heatwave characteristics.

This research uses new Shared Socioeconomic Pathways (SSP)-based scenarios, which considers economic and social factors alongside emissions and land use changes. The SSPs represent a refined version of the CMIP5 RCP

ZHOU ET AL. 3 of 13

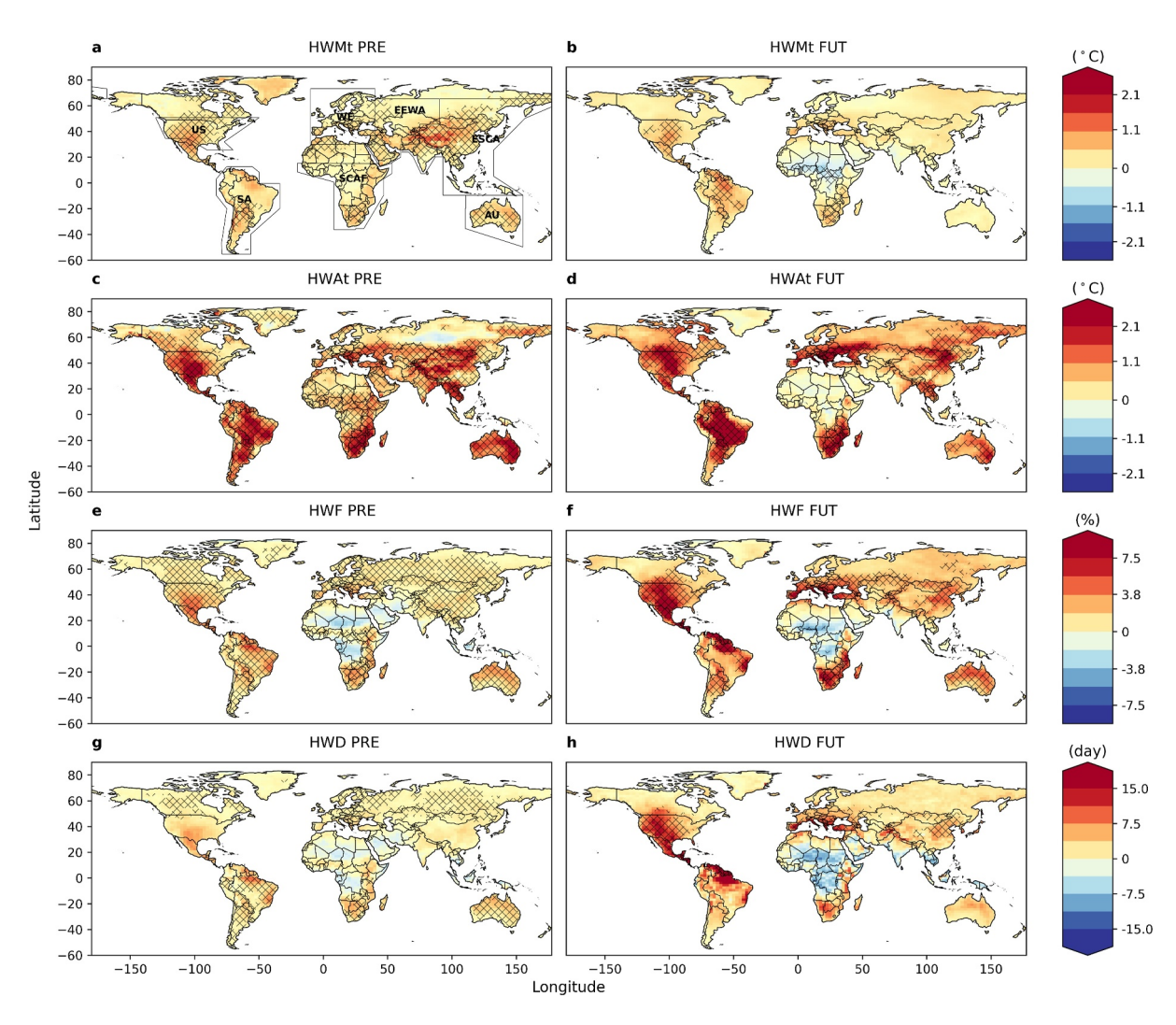


Figure 1. Spatial distributions of changes in soil moisture effects on different heatwave characteristics. (a, c, e, and g), Differences between CTL and pdLC for the heatwave characteristics such as heatwave mean intensity (a; HWMt), peak intensity (c; HWAt), frequency (e; HWF), and duration (g; HWD) is depicted in 2000–2030 (PRE). (b, d, f, and h), Differences between CTL and pdLC for the heatwave characteristics such as heatwave mean intensity (b; HWMt), peak intensity (d; HWAt), frequency (f; HWF), and duration (h; HWD) in 2040–2070 (FUT). The data within this figure are of SSP585. Hatching indicates where the differences between CTL and pdLC are statistically significant (KS test, p value < 0.05). The analysis is limited to the summer-centering periods. The extensions in color bars indicate values beyond the limits. Oceans have been masked in white.

scenarios, now incorporating socioeconomic factors and produced with the latest versions of integrated assessment models (IAMs). CMIP6 climate projections utilize upgraded climate models, drawing upon recent data regarding emission trends (O'Neill et al., 2016). Enhancements have also been made to the land surface components of climate models subsequent to those in CMIP5 (Boucher et al., 2020; Döscher et al., 2022; Eyring et al., 2016; Lurton et al., 2020; Mauritsen et al., 2019; Tatebe et al., 2019). The study focuses on two specific scenarios: SSP126, which assumes strong climate action and aims to limit warming to 2°C, and SSP585, which represents a high-emission future with significant warming.

3. Data

3.1. CMIP6 Data

To quantify soil moisture effects under different warming scenarios, we employed historical experiment, the Scenario Model Intercomparison Project (ScenarioMIP) (O'Neill et al., 2016; Tebaldi et al., 2021), and the LFMIP-pdLC of the Land Surface, Snow and Soil moisture Model Intercomparison (LS3MIP) (van den Hurk et al., 2016) in CMIP6 (Eyring et al., 2016). Due to (a) the removed impacts from soil moisture trend at

ZHOU ET AL. 4 of 13

multidecadal time scales and (b) the removed short-term S-T interactions at interannual and sub seasonal time scales in LFMIP-pdLC, the results of historical with ScenarioMIP (in the following text we refer it to CTL) minus pdLC can be used to indicate effects from soil moisture changes. For consistency, climate model data sets have been interpolated into a common grid of 2.5° longitude by 1.875° latitude using a conservative remapping approach (Schulzweida, 2023). The interpolation makes it feasible to use multi-model ensemble mean of climate models in this research.

3.2. Population Data Set and Exposure

As population exposure depends on both population attributes and heatwave characteristics, the trend of future population is considered as well in our research to constrain uncertainties in simulating changes of population exposure to heatwaves. In this way, gridded data of global population count for the year 2000, 2010, 2020, 2030, 2040, 2050, 2060, and 2070, are used in this project to investigate population exposure to heatwaves (Jones & O'Neill, 2016, 2020). In the data set, base year is 2000 and population projections are consistent both quantitatively and qualitatively with the SSPs, in which the projection data in both SSP1 and SSP5 are used in this project. The spatial resolution of this data set is 0.125° longitude by 0.125° latitude. To reconcile the spatial resolution and grid availability in climate and population projections, we calculate $2.5^{\circ} \times 1.875^{\circ}$ population grids by aggregating the total population within the $1/8^{\circ} \times 1/8^{\circ}$ population grids that fall within the domain of each climate grid (Schulzweida, 2023). The interpolation enables quantifications of population exposure to heatwaves, which is calculated as the following:

$$\Delta PE = P_{\text{fut}}/P_{\text{allf}} - P_{\text{pre}}/P_{\text{allp}} \tag{2}$$

In a certain region, ΔPE indicates the change of population exposure, $P_{\rm fut}$ indicates the future population count above a certain threshold of one heatwave characteristic, $P_{\rm pre}$ indicates the current population count above a certain threshold of the heatwave characteristic. $P_{\rm allf}$ is the average of the global population count values in 2040, 2050, 2060, and 2070, $P_{\rm allp}$ is the average of the global population count values in 2000, 2010, 2020, and 2030.

At each grid within the map (Figure 3), the value of the population exposure is the average of those for the four different heatwave characteristics. For quantifying population exposure to different heatwave characteristics in the seven domains, we first aggregated population of all the grids for a specific domain and then calculated the population exposure for each heatwave characteristic.

3.3. Definition of Domains

To better characterize regional soil moisture effects, we use the updated Intergovernmental Panel on Climate Change Sixth Assessment Report (IPCC AR6) climate reference regions, which are identified according to consistent regional climate features using observational and modeling (CMIP6) climate data sets (Iturbide et al., 2020).

Seven domains from the major habitable continents are set for this study: East, North, South, Southeast and central Asia (ESCA); Australia (AU); the US; West Europe (WE); East Europe and West Asia (EEWA); Southern and central Africa (SCAF, African continent south of the Sahara Desert); and South America (SA). The Eurasia has been divided into three parts: ESCA, WE, and EEWA.

4. Results

4.1. Changes in Soil Moisture Effects on Heatwaves

Figure 1 illustrates that the effects of incorporating soil moisture variability and trend are diverse in the forms of four heatwave characteristics (HWMt, HWAt, HWF, and HWD) across the world (Figure 1). Differences of soil moisture between pdLC and CTL lead to more increases in all the heatwave characteristics in the future period across the US, SA, WE, East Europe, northern Asia, eastern Asia, southern and southeastern Africa (Figure 1).

In middle Africa and Australia instead, the changes of the soil moisture effects on heatwave characteristics are mostly negative. Transitions from either less decreases or even increases of heatwave characteristics to (more) decreases are found over these two regions (except for HWF in Australia Figures 1e and 1f).

ZHOU ET AL. 5 of 13

23284277, 2024, 7, Downloaded

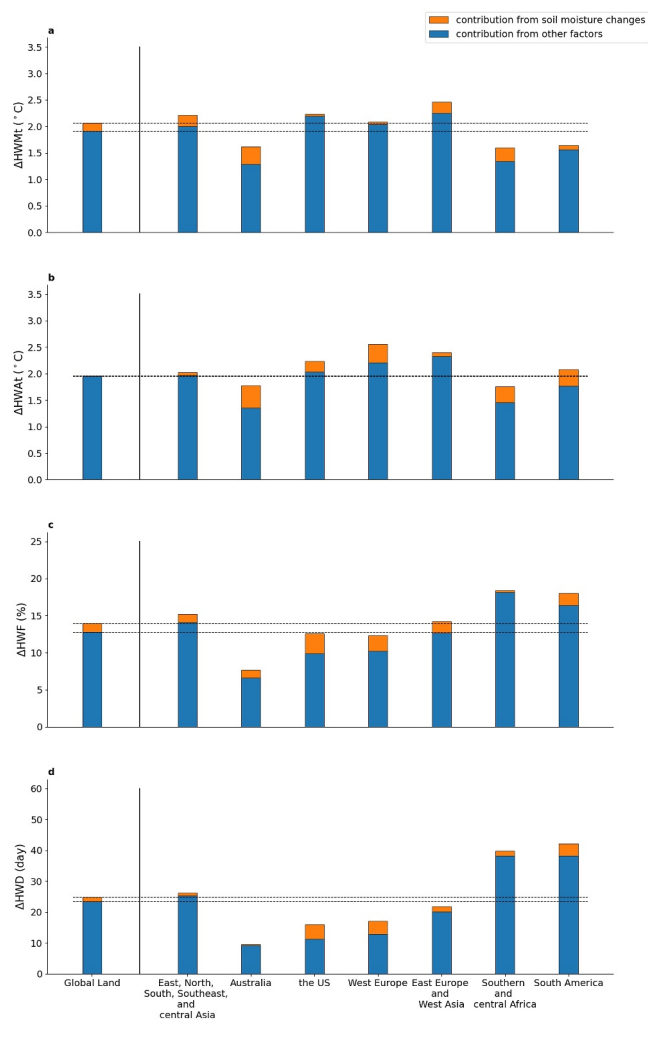


Figure 2. Projected changes in global and regional heatwave characteristics. (a–d) Increases of heatwave mean intensity (a; HWMt), peak intensity (b; HWAt), frequency (c; HWF), and duration (d; HWD) induced by soil moisture changes and other factors under SSP585 are displayed across two 30-year periods. The global and regional values of the projected changes shown here are area-weighted. The changes are between 2040–2070 and 2000–2030. The orange part indicates contributions of soil moisture changes; the blue part indicates other factors. The domains are delineated in both Figures 1 and 3, the oceans are excluded for these domains. Horizontal bars are added to this figure to help readers more easily compare the increases of global and regional heatwave characteristics with or without contributions from soil moisture.

4.2. Soil Moisture Contributions to Projected Changes in Heatwaves

Heatwaves tend to be longer, more intense, and affecting more land regions by the end of the century when including the effects of soil moisture (Figure 2). SCAF and SA are projected to experience longer and more frequent heatwaves in contrast to other domains (Figures 2c and 2d). As heatwave frequency and duration are functions of the underlying temperature distributions, in these regions, the 90th percentile can be surpassed by a smaller change in temperature as the temperature distribution is much narrower and has a larger fraction of higher temperature values compared to that in the midlatitudes. Besides, one of the other reasons is that tropical and extratropical regions tend to have the largest changes heatwave frequency and duration (Figures S4e-S4h in Supporting Information S1) and the two domains (SA and SCAF) have more tropical and extra-tropical grid cells. By contrast, high-latitude regions tend to have the largest changes in heatwave magnitude and amplitude (Figures S4a–S4d in Supporting Information S1). The three domains (US, WE, and EEWA) have more high-latitude grid cells, therefore, increases of heatwave magnitude and amplitude are much greater in US, WE, and EEWA compared to other domains (Figures 2a and 2b). In the meantime, as grids in ESCA are widely distributed among all the latitudes and those in AU are distributed in mid-latitude regions where none of the heatwave characteristics increase greatly (Figure S4 in Supporting Information S1), ESCA tends to have relatively higher projected changes of all the heatwave characteristics compared with other domains while those in AU are less.

Contributions from soil moisture to the four heatwave characteristics are different. In AU, even though projected changes of all the heatwave characteristics are less compared to other domains, soil moisture effects take up more percentage in total changes in all the heatwave characteristics except heatwave duration (Figure 2). In contrast to other domains, soil moisture effects are stronger (more than 0.1°C) in controlling the increases of heatwave mean intensity in ESCA, AU, EEWA, and SCAF (Figure 2a), the role of S-T coupling is stronger in inducing more increases (more than 0.15°C) for the intensity of the hottest heatwaves in AU, WE, SCAF, and SA (Figure 2b). Compared with other domains, contributions from soil moisture to heatwave frequency and duration are greater in US, WE, EEWA, and SA, as they induce an increase of 1%-3% in heatwave frequency for these domains (Figure 2c) and an extension of up to 4 days in the duration of the longest yearly heatwave (Figure 2d). Additionally, SCAF is the only domain where contributions from soil moisture to increases of heatwave frequency is less than 0.5%.

Soil moisture constitutes an important component in projected changes of all the four heatwave characteristics. Regional differences in influences from soil moisture especially long-term soil moisture trend contribute to

different changes of the heatwave characteristics in the seven domains. Even though soil moisture contributions are not great in some of the four heatwave characteristics among those domains, soil moisture is found to be especially detectable in the seven chosen domains in the perspectives of at least two heatwave characteristics. When comparing with global average (Figure 2), most domains get more contributions from soil moisture changes (e.g., all of domains in the perspective of HWAt; all the domains excluding AU and SCAF in HWF; all of the domains apart from ESCA and AU in HWD), these domains in this way can be called heatwave hotspots where soil moisture changes are more important in amplifying heatwave conditions compared to other places in the world.

ZHOU ET AL. 6 of 13

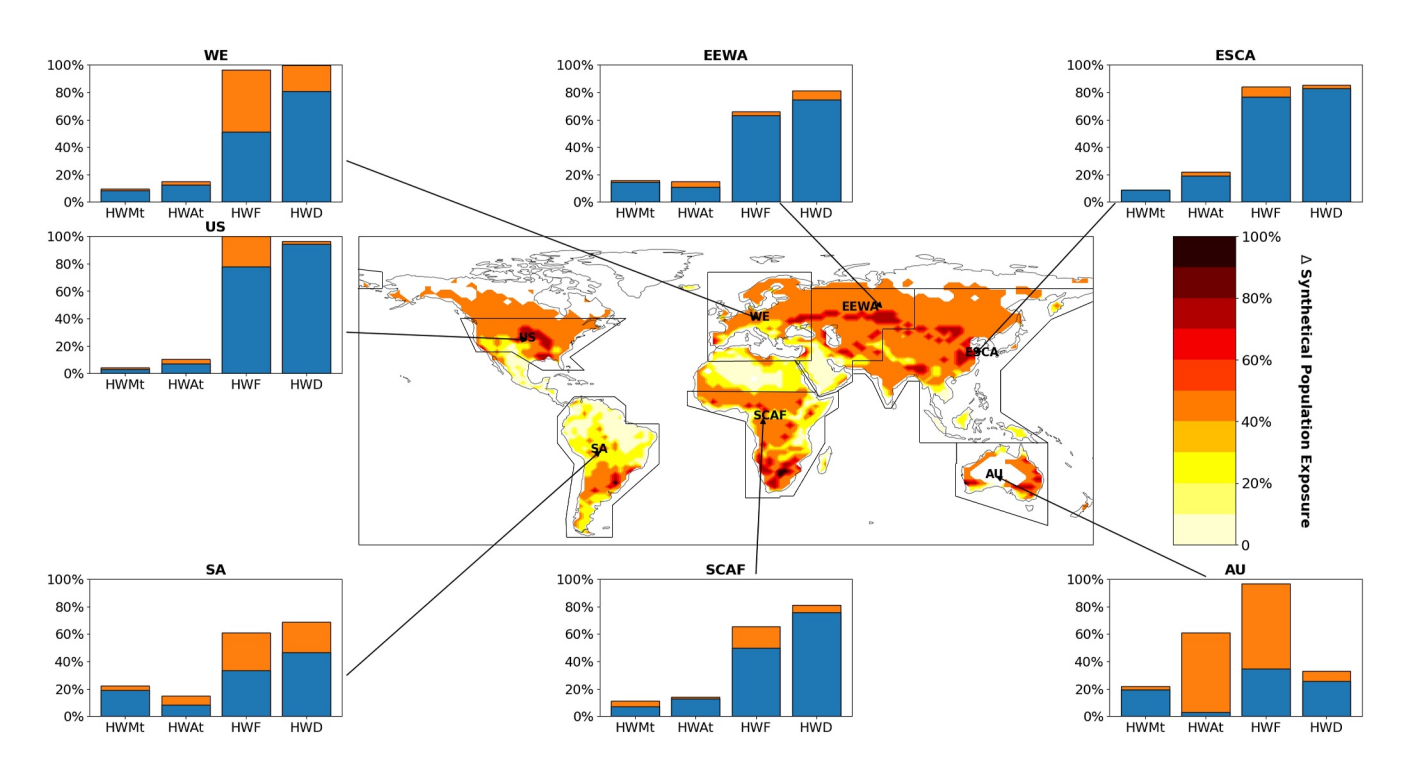


Figure 3. Projected changes of population exposure to heatwaves. Increases of heatwaves' impacts on the human population induced by soil moisture changes and other factors under SSP585 are shown in the form of four different heatwave characteristics, which includes heatwave mean intensity (HWMt), peak intensity (HWAt), frequency (HWF), and duration (HWD). The changes are between present period (2040–2070) and future period (2000–2030) and are calculated between the population percentage that is above the threshold (HWMt, 21.5°C; HWAt, 32°C; HWF, 5%; HWD, 9 days) in both 2000–2030 and 2040–2070. The population data for the current period are of 2000–2030, while those in the future period are of 2040–2070. The map indicates the synthetical increases of the population exposure based on the four heatwave characteristics. In the bar plots, the orange part indicates contributions from soil moisture changes; the blue part indicates other factors. Oceans and other regions without population data available have been masked in white.

4.3. Population Exposure to Heatwaves

Changes of population exposure to heatwaves, and the role of soil moisture in defining that exposure are also investigated in this study. Population percentage that is above the threshold (HWMt, 21.5°C; HWAt, 32°C; HWF, 5%; HWD, 9 days) in both present period (2000–2030) and future period (2040–2070) are compared to calculate changes of the population exposure. It is found that large increases in population exposure by the end of the century, which commonly reaches 50% based on the four heatwave characteristics, are distributed widely across the hotspots. To be specific, northern and northeastern parts of the US, southern part of the SA, SCAF excluding the eastern part, WE excluding the Mediterranean part, EEWA excluding the Arabian Peninsula, ESCA excluding Southeast Asia, and AU will experience a great increase (more than 50%) in population exposure to heatwave impacts (Figure 3). By contrast, a different phenomenon was found in Central America, Amazon region, Mediterranean region, Arabian Peninsula, and eastern part of SCAF, where most of the parts in this region will experience less increases (less than 30%) in population exposure to heatwave impacts (Figure 3). In those regions, soil moisture generally tends to incur a great positive increase in most of the heatwave characteristics (Figures 1a, 1c, 1e, and 1g) in the present period, which facilitates that most of the population in these regions are exposed to heatwave impacts above the thresholds under current period and the future increases in population exposure to heatwave impacts are not evident. Furthermore, Sahara region and Southeast Asia are also two regions where increases of population exposure to heatwaves (less than 20%) are less than other hotspots. These are the regions where most of the population have already been exposed to heatwave impacts above the thresholds even though the soil moisture impacts are not pronounced (Figures 1a, 1c, 1e, and 1g).

In all the selected domains (ESCA, EEWA, WE, SA, US, and SCAF) except AU, increases in population exposure to heatwave frequency, and duration are the greatest (which are normally more than 60%) among all the five heatwave characteristics (Figure 3). For heatwave mean intensity and peak intensity, increases of population exposure to both heatwave characteristics are similar and also less (less than 25%) compared to the other two

ZHOU ET AL. 7 of 13

heatwave characteristics in all the domains except AU (Figure 3). Increases of heatwave frequency and duration are both greater than those of heatwave magnitude and amplitude in terms of values (Figure S4 in Supporting Information S1). Therefore, increases of population exposed to heatwave frequency and duration across their thresholds tend to happen in more places, which serves as one reason for the phenomenon where increases of population exposure to heatwave frequency and duration are greater than those to the other two heatwave characteristics.

Soil moisture changes tend to make more contributions to increases of population exposure to heatwaves in WE, AU, SA, SCAF, and US (Figure 3). By contrast, in EEWA and ESCA, soil moisture changes contribute a minor component to increases of population exposure to heatwaves in the perspectives of all the four heatwave characteristics (Figure 3). Moreover, in all the selected domains other than AU, S-T coupling is also found to make less contributions to increases of population exposure to heatwave mean intensity and amplitude (Figure 3). Nevertheless, soil moisture still takes a great component in projected changes of heatwave magnitude and amplitude in US, SA, SCAF, AU, and EEWA.

5. Conclusions

Our study shows the influences from the changes in soil moisture on heatwave conditions by isolating soil moisture influences and comparing the future and present responses of extreme indices to soil moisture. The influences of soil moisture include both the effects of short-term variability and climate change-induced longterm changes of soil moisture on heatwaves. This study focused on the near future period (2040-2070) to project changes from current period (2000-2030), reflecting approaching challenges faced for implementing mitigation strategies and global policies against imminent heatwave impacts. It is found that heatwaves are projected to increase in their frequency, duration, mean intensity, and peak intensity for most mid-latitude land regions by the end of the 21st century (Figure S4 in Supporting Information S1). Moreover, greater increases are found over tropical and extra-tropical regions for heatwave frequency and duration, while for heatwave magnitude and amplitude, greater increases happen in the high-latitude regions (Figure S4 in Supporting Information S1). It is found that soil moisture effects are stronger in US, SA, WE, East Europe, northern Asia, eastern Asia, SCAF, and AU (Figure 1). The regions with the largest responses of heatwave characteristics to S-T coupling are majorly distributed in mid-latitude areas in both hemispheres (Figure 1), which coincide with most of those identified with strong impacts from projected changes of soil moisture (Figure S4 in Supporting Information S1; Seneviratne et al., 2013). The areas in our study that are identified with strong contributions of soil moisture to heatwaves (Figure 1) tend to agree with some observationally derived estimates (M. Hirschi et al., 2010; Mueller & Seneviratne, 2012). Besides, some former modeling studies have also indicated regional differences in S-T coupling (Knist et al., 2017; Seneviratne et al., 2006).

Soil moisture changes constitute a strong component in the exacerbation of heatwaves in ESCA, AU, US, WE, EEWA, SCAF, and SA. Compared with global average, more contributions from soil moisture changes are found over most of these domains (Figure 2). It confirms the results of some existing research that removing S-T coupling will significantly weaken the temperature extremes over most land surfaces (Lorenz et al., 2016; Vogel et al., 2017).

The intensification of heatwaves due to soil moisture is more concentrated in densely populated regions (Figures 1 and 2), which makes these dynamics especially salient both in real-world scenarios and in their simulation. In our investigations on changes of population exposure to heatwaves and how the soil moisture influences those, we found large increases (more than 50%) of population exposure to heatwaves in northern and northeastern parts of the US, southern part of the SA, SCAF excluding the eastern part, WE excluding the Mediterranean part, EEWA excluding the Arabian Peninsula, ESCA excluding Southeast Asia, and AU (Figure 3). These regions excluding AU are also located in the regions where soil moisture effects are strong (Figure 1) and most of them are densely populated regions. However, soil moisture effects sometimes don't match in their contributions to changes of heatwave characteristics and those of population exposure to heatwaves. For example, in AU, although soil moisture effects are not strong enough to make a dominant component in contributing to increases of heatwave amplitude and frequency, they make significant impacts on increasing population exposure to both heatwave characteristics. One of the reasons is that the calculation of population exposure to heatwaves utilize only population count even though population exposure to heatwaves incorporates both population count and heatwave metrics. While comparatively less population count is distributed in some subregions with less soil moisture

ZHOU ET AL. 8 of 13

effects, other parts in the same domain where population count that is above the respective threshold tends to change greatly are sometimes limited to the regions with stronger soil moisture effects (Figure 1), which makes the contributions of soil moisture to changes of population exposure greater than those to projected changes of heatwave characteristics. Using percentage of population count to express exposure to heatwave cause underestimation of heatwave impacts such that for specific regions increases of population count exposed to heatwaves alone don't necessarily induce increases in percentage of population count exposed to heatwaves. That said, increases of population exposure to heatwave frequency and duration are found to be strong, which indicates that different heatwave characteristics can be incorporated in heatwave evaluation and more emphases should be put on these two heatwave characteristics in the future when considering policies addressing heatwave impacts on humans. In summary, understanding soil moisture dynamics and its influence on heatwaves is essential for effective heatwave management and public health strategies. Better simulation of soil moisture data can improve heatwave predictions, thus allowing for better public health preparedness.

As SSP126 represents a low emission scenario, which serves as a more optimistic future reference compared with the challenging SSP585. It is helpful in more completely understanding results of incorporating soil moisture variability and trend on heatwave impacts by comparing both scenarios. Even though S-T coupling is generally less strong (Figure 1 and Figure S1 in Supporting Information S1), it generally makes up relatively higher percentage (Figure 2 and Figure S2 in Supporting Information S1) of less projected changes of all the heatwave characteristics (Figures S4 and S5 in Supporting Information S1) in SSP126 in contrast to SSP585. Contribution from soil moisture effects to increases of population exposure to different heatwave characteristics are relatively similar in SSP126 and SSP585, while projected increases of population exposure to heatwave characteristics are different in the two scenarios (Figure 3 and Figure S3 in Supporting Information S1). One of the reasons is that the change measured for population exposure is in percentage based on the four heatwave characteristics rather than in population count and increases of the population exposed to heatwaves across the thresholds in SSP585 happen less than those in SSP126 (Figures S6 and S7 in Supporting Information S1), which makes the increases of population exposure in SSP585 less than those in SSP126.

Some land management can be implemented to mitigate the impacts of heatwaves on human population. In particular, as irrigation can greatly change local soil moisture, it can be seen as one of the plausible approaches to alleviate heat extremes (A. L. Hirsch et al., 2017; Thiery et al., 2020). Irrigation can substantially reduce human exposure (0.79–1.29 billion) to heatwaves (Thiery et al., 2020). However, although irrigation is found to decrease temperature in some places (A. L. Hirsch et al., 2017; Thiery et al., 2020), it is proved not to attenuate or even increase moist heat stress while increasing air humidity (Krakauer et al., 2020; Wouters et al., 2022). In addition, ample water supply is a challenge especially at some hot regions where water availability is sometimes limited (Barker et al., 2021; He et al., 2021), which raises practical issues for using irrigation as an adaption option against heatwaves. Apart from irrigation, some other land management, such as land radiative management and forestation can be taken into consideration (Gormley-Gallagher et al., 2022; Kala et al., 2022; Portmann et al., 2022; Seneviratne et al., 2018), for example, the study conducted by A. L. Hirsch et al. (2017) has indicated the collective effects of both irrigation and crop albedo were robust in cooling the land surface, which can reduce hot temperature extremes by more than 2°C in North America, Eurasia, and India compared to a scenario in which no land management is implemented (A. L. Hirsch et al., 2017). The land radiative management was found to help counteract hot extremes especially in densely populated and some agricultural regions (Seneviratne et al., 2018). Regional land radiative management reduces average temperature anomaly during heatwaves by 0.8–1.2°C and heatwave frequency by 10-20 days over Europe and North America (Kala et al., 2022).

Future investigations on influences from sole background warming trend are needed. Climatic warming trend may dominate changes of regional temperature compared to soil moisture, land use changes, or other land-atmosphere interactions (Perkins-Kirkpatrick & Lewis, 2020; Pitman et al., 2011). Land-atmosphere coupling regime and its variability are also one of the future research focuses (Denissen et al., 2022; Hsu & Dirmeyer, 2023). Furthermore, occurrence and severity of heatwaves and their future changes under multiple compounding drivers deserve further research. In addition to soil moisture effects, heatwave evolution and variability are also related to natural climate variability such as El Niño Southern Oscillation (ENSO) and Indian Ocean Dipole (IOD). These potential drivers will evolve over time and alter the risk of future heatwaves. Taking climate indices as covariates or using sensitivity experiments based on model simulations can shed light on the effects of changes in natural variability and their corresponding impacts on occurrence and severity of future heatwaves.

ZHOU ET AL. 9 of 13

The subregions divided from the domains need to be investigated in the future research to improve evaluation of population exposure to heatwaves. Different regional thresholds in measuring population exposure to heatwaves need to be considered in the future studies. Different effects from soil moisture on subregions are required for further studies, for example, southern and southeastern Africa and middle Africa have contrasting trends of the soil moisture effects on heatwave characteristics, the Arabian Peninsula and East Europe have similar phenomena (Figure 1). In the meantime, Southeast Asia, northern Asia, eastern Asia, middle Asia, northern India, and southern India all have different patterns of heatwaves from soil moisture effects, and among these subregions, S-T coupling on different heatwave characteristics is varied if diving into a more local scale. For subregions such as Arctic regions in Russia, Far East in Russia, Tibetan Plateau, the impacts of heatwaves measured through increases of population exposure are mild from a population perspective as these regions have low population count. However, the exacerbation of heatwave conditions to these regions will still cause catastrophic impacts on the local ecosystems as the ecosystems in these regions are fragile and extremely vulnerable to climate change. More future studies on regional differences of heatwave impacts, which may integrate finer spatial resolutions of climate model results and recent historical simulations on spatial distributions of soil moisture effects, heatwave characteristics, and human populations, are needed to better find local thresholds of heatwave characteristics and account for the local changes of human exposure to heatwaves.

Different regions also require tailored analysis periods. A pronounced seasonal pattern occurs over higher latitudes, with heat extremes more common in June through August (JJA) in the Northern Hemisphere and December through February (DJF) in the Southern Hemisphere. On the other hand, tropical regions experience a more uniform distribution of extreme heat events throughout the year, with the most intense dry heat occurring in varying months, as noted by Rogers et al. (2021). Tomasini et al. (2022) observed that during April 2010, the West Sahel experienced its peak season for heatwaves coinciding with the culmination of the dry season, when the impacts of soil moisture on temperature through land-atmosphere feedbacks might be small (Tomasini et al., 2022). Additionally, recognizing distinct seasons for heatwaves in various regions, along with the patterns of monsoon, aids in examining how soil moisture might interact with humid heat extremes in future studies (Birch et al., 2022; Rogers et al., 2021).

Contrast between urban area and non-urban area is also a focal point to be considered. Rapid urbanization process is expected in the future, which tends to make urban heatwaves more frequent and increases the population exposure to these events through urban heat island and some other feedbacks (Han et al., 2021; Wang et al., 2021). At the urban scale the feedbacks such as urban heat island effects that cause urban heatwaves are not well resolved by most current global-scale climate models. These feedbacks are not negligible as they can augment heatwave conditions and add uncertainty to our estimations (Zheng et al., 2021). Moreover, populations are not equally exposed to heatwaves, population in some regions may have access to advanced cooling systems, well-insulated buildings, or green spaces which reduce surrounding temperature, while the others may not. Such inequality of access to cooling services are exacerbated by the decreases of the cooling services per se. For example, study carried out by Dong et al. (2022) showed that approximately 93.3% of the cities they investigated had significant decreasing trends of the urban green spaces (Dong et al., 2022).

Same heatwave temperature threshold (T_{90}) throughout the present period of 2000–2030 and future period of 2040– 2070 contributes partly to the situation where all the selected heatwave characteristics increased significantly (Figure 2, Figures S4 and S5 in Supporting Information S1). Changes in both spatial and temporal dimensions of heatwayes strongly depend on the selected threshold as strong increases in heatwaye characteristics are detected if time-invariant climatic thresholds are adopted while minor changes are found in these characteristics when moving thresholds are defined (Vogel et al., 2020). Even though time-invariant climatic thresholds have been utilized to investigate land contributions to temperature extremes in numerous former studies (Coumou & Robinson, 2013; Lorenz et al., 2010; Perkins, 2015), moving thresholds can be more widely utilized in the future studies.

Data Availability Statement

Gridded data of global population count are available from Socioeconomic Data and Applications Center of National Aeronautics and Space Administration (NASA) (Jones & O'Neill, 2020). The CMIP6 model simulations are from Earth System Grid Federation (Boucher et al., 2018, 2019a, 2019b, 2019c; Consortium, 2019a, 2019b, 2019c, 2020; Onuma & Kim, 2021; Shiogama et al., 2019a, 2019b; Stacke et al., 2019; Tatebe & Watanabe, 2018;

ZHOU ET AL. 10 of 13 Wieners et al., 2019a, 2019b, 2019c). Related processing, analysis, and plotting codes as well as some intermediate data for plotting the figures can be found through J. Zhou et al. (2024).

Acknowledgments

We extend our gratitude to the World Climate Research Programme and its working group on coupled modeling for coordinating and advancing CMIP6. We also express appreciation to the climate modeling groups for generating and sharing their model outputs, as well as to the Earth System Grid Federation for storing the data and facilitating access. Additionally, we thank the various funding agencies that support both CMIP6 and ESGF. J. Z. is supported by China Scholarship Council.

References

- Barker, A., Pitman, A., Evans, J. P., Spaninks, F., & Uthayakumaran, L. (2021). Drivers of future water demand in Sydney, Australia: Examining the contribution from population and climate change. *Journal of Water and Climate Change*, 12(4), 1168–1183. https://doi.org/10.2166/wcc. 2020.230
- Birch, C. E., Jackson, L. S., Finney, D. L., Marsham, J. M., Stratton, R. A., Tucker, S., et al. (2022). Future changes in African heatwaves and their drivers at the convective scale. *Journal of Climate*, 35(18), 5981–6006. https://doi.org/10.1175/jcli-d-21-0790.1
- Boucher, O., Denvil, S., Levavasseur, G., Cozic, A., Caubel, A., Foujols, M.-A., et al. (2018). IPSL IPSL-CM6A-LR model output prepared for CMIP6 CMIP historical [Dataset]. https://doi.org/10.22033/ESGF/CMIP6.5195
- Boucher, O., Denvil, S., Levavasseur, G., Cozic, A., Caubel, A., Foujols, M.-A., et al. (2019a). IPSL IPSL-CM6A-LR model output prepared for CMIP6 ScenarioMIP ssp126 [Dataset]. https://doi.org/10.22033/ESGF/CMIP6.5262
- Boucher, O., Denvil, S., Levavasseur, G., Cozic, A., Caubel, A., Foujols, M.-A., et al. (2019b). IPSL IPSL-CM6A-LR model output prepared for CMIP6 ScenarioMIP ssp585 [Dataset]. https://doi.org/10.22033/ESGF/CMIP6.5271
- Boucher, O., Denvil, S., Levavasseur, G., Cozic, A., Caubel, A., Foujols, M.-A., et al. (2019c). IPSL IPSL-CM6A-LR model output prepared for CMIP6 LS3MIP amip-lfmip-pdLC [Dataset]. https://doi.org/10.22033/ESGF/CMIP6.5122
- Boucher, O., Servonnat, J., Albright, A. L., Aumont, O., Balkanski, Y., Bastrikov, V., et al. (2020). Presentation and evaluation of the IPSL-CM6A-LR climate model. *Journal of Advances in Modeling Earth Systems*, 12(7). https://doi.org/10.1029/2019ms002010
- Consortium, E.-E. (2019a). EC-Earth-Consortium EC-Earth3 model output prepared for CMIP6 CMIP historical [Dataset]. https://doi.org/10.22033/ESGF/CMIP6.4700
- Consortium, E.-E. (2019b). EC-Earth-Consortium EC-Earth3 model output prepared for CMIP6 ScenarioMIP ssp126 [Dataset]. https://doi.org/10.22033/ESGF/CMIP6.4874
- Consortium, E.-E. (2019c). EC-Earth-Consortium EC-Earth3 model output prepared for CMIP6 ScenarioMIP ssp585 [Dataset]. https://doi.org/10.22033/ESGF/CMIP6.4912
- Consortium, E.-E. (2020). EC-Earth Consortium (EC-Earth) (2020). EC-Earth-Consortium EC-Earth3 model output prepared for CMIP6 LS3MIP
- amip-lfmip-pdLC [Dataset]. https://doi.org/10.22033/ESGF/CMIP6.4542
 Coumou, D., & Robinson, A. (2013). Historic and future increase in the global land area affected by monthly heat extremes. *Environmental*
- Research Letters, 8(3), 034018. https://doi.org/10.1088/1748-9326/8/3/034018

 Cowan, T., Purich, A., Perkins, S. E., Pezza, A., Boschat, G., & Sadler, K. (2014). More frequent, longer, and hotter heat waves for Australia in the
- twenty-first century. Journal of Climate, 27(15), 5851–5871. https://doi.org/10.1175/jcli-d-14-00092.1
- Denissen, J. M. C., Teuling, A. J., Pitman, A. J., Koirala, S., Migliavacca, M., Li, W., et al. (2022). Widespread shift from ecosystem energy to water limitation with climate change. *Nature Climate Change*, 12(7), 677–684. https://doi.org/10.1038/s41558-022-01403-8
- Dirmeyer, P. A., Balsamo, G., Blyth, E. M., Morrison, R., & Cooper, H. M. (2021). Land-atmosphere interactions exacerbated the drought and heatwave over northern Europe during summer 2018. *AGU Advances*, 2(2), e2020AV000283. https://doi.org/10.1029/2020av000283
- Dong, Y., Ren, Z., Fu, Y., Hu, N., Guo, Y., Jia, G., & He, X. (2022). Decrease in the residents' accessibility of summer cooling services due to green space loss in Chinese cities. *Environment International*, 158, 107002. https://doi.org/10.1016/j.envint.2021.107002
- Döscher, R., Acosta, M., Alessandri, A., Anthoni, P., Arsouze, T., Bergman, T., et al. (2022). The EC-Earth3 Earth system model for the coupled model intercomparison project 6. Geoscientific Model Development, 15(7), 2973–3020. https://doi.org/10.5194/gmd-15-2973-2022
- Eyring, V., Bony, S., Meehl, G. A., Senior, C. A., Stevens, B., Stouffer, R. J., & Taylor, K. E. (2016). Overview of the coupled model inter-comparison project phase 6 (CMIP6) experimental design and organization. *Geoscientific Model Development*, 9(5), 1937–1958. https://doi.org/10.5194/gmd-9-1937-2016
- Fischer, E. M., Seneviratne, S. I., Vidale, P. L., Lüthi, D., & Schär, C. (2007). Soil moisture–atmosphere interactions during the 2003 European summer heat wave. *Journal of Climate*, 20(20), 5081–5099. https://doi.org/10.1175/jcli4288.1
- Geirinhas, J. L., Russo, A. C., Libonati, R., Miralles, D. G., Sousa, P. M., Wouters, H., & Trigo, R. M. (2022). The influence of soil dry-out on the record-breaking hot 2013/2014 summer in Southeast Brazil. Scientific Reports, 12(1), 5836. https://doi.org/10.1038/s41598-022-09515-z
- Gormley-Gallagher, A. M., Sterl, S., Hirsch, A. L., Seneviratne, S. I., Davin, E. L., & Thiery, W. (2022). Agricultural management effects on mean and extreme temperature trends. Earth System Dynamics, 13(1), 419–438. https://doi.org/10.5194/esd-13-419-2022
- Han, L., Yu, X., Xu, Y., Deng, X., Yang, L., Li, Z., et al. (2021). Enhanced summertime surface warming effects of long-term urbanization in a humid urban agglomeration in China. *Journal of Geophysical Research: Atmospheres*, 126(21), e2021JD035009. https://doi.org/10.1029/2021jd035009
- Hauser, M., Orth, R., & Seneviratne, S. I. (2016). Role of soil moisture versus recent climate change for the 2010 heat wave in western Russia. Geophysical Research Letters, 43(6), 2819–2826. https://doi.org/10.1002/2016gl068036
- He, C., Liu, Z., Wu, J., Pan, X., Fang, Z., Li, J., & Bryan, B. A. (2021). Future global urban water scarcity and potential solutions. *Nature Communications*, 12(1), 4667. https://doi.org/10.1038/s41467-021-25026-3
- Hirsch, A. L., Evans, J. P., Virgillio, G. D., Perkins-Kirkpatrick, S., Argüeso, D., Pitman, A. J., et al. (2019). Amplification of Australian heatwaves via local land-atmosphere coupling. *Journal of Geophysical Research: Atmospheres*, 124(24), 13625–13647. https://doi.org/10.1029/2019jd030665
- Hirsch, A. L., & King, M. J. (2020). Atmospheric and land surface contributions to heatwaves: An Australian perspective. *Journal of Geophysical Research: Atmospheres*, 125(17), e2020JD033223. https://doi.org/10.1029/2020jd033223
- Hirsch, A. L., Wilhelm, M., Davin, E. L., Thiery, W., & Seneviratne, S. I. (2017). Can climate-effective land management reduce regional warming? *Journal of Geophysical Research: Atmospheres*, 122(4), 2269–2288. https://doi.org/10.1002/2016jd026125
- Hirschi, M., Seneviratne, S. I., Alexandrov, V., Boberg, F., Boroneant, C., Christensen, O. B., et al. (2010). Observational evidence for soil-moisture impact on hot extremes in southeastern Europe. *Nature Geoscience*, 4(1), 17–21. https://doi.org/10.1038/ngeo1032
- Hodges, J. L. (1958). The significance probability of the Smirnov two-sample test. *Arkiv för Matematik*, *3*(5), 469–486. https://doi.org/10.1007/bf02589501
- Hsu, H., & Dirmeyer, P. A. (2023). Soil moisture-evaporation coupling shifts into new gears under increasing CO₂. *Nature Communications*, 14(1), 1162. https://doi.org/10.1038/s41467-023-36794-5
- Hudson, D., & Marshall, A. G. (2016). Extending the Bureau's heatwave forecast to multi-week timescales.

ZHOU ET AL. 11 of 13

- Iturbide, M., Gutiérrez, J. M., Alves, L. M., Bedia, J., Cerezo-Mota, R., Cimadevilla, E., et al. (2020). An update of IPCC climate reference regions for subcontinental analysis of climate model data: Definition and aggregated datasets. Earth System Science Data, 12(4), 2959–2970. https://doi.org/10.5194/essd-12-2959-2020
- Jones, B., & O'Neill, B. C. (2016). Spatially explicit global population scenarios consistent with the Shared Socioeconomic Pathways. Environmental Research Letters, 11(8), 084003. https://doi.org/10.1088/1748-9326/11/8/084003
- Jones, B., & O'Neill, B. C. (2020). Global one-eighth degree population base year and projection grids based on the shared socioeconomic pathways, revision 01 [Dataset]. https://sedac.ciesin.columbia.edu/data/collection/gpw-v4
- Jones, B., Tebaldi, C., O'Neill, B. C., Oleson, K. W., & Gao, J. (2018). Avoiding population exposure to heat-related extremes: Demographic change vs climate change. Climatic Change, 146(3-4), 423-437. https://doi.org/10.1007/s10584-017-2133-7
- Kala, J., Hirsch, A. L., Ziehn, T., Perkins-Kirkpatrick, S. E., De Kauwe, M. G., & Pitman, A. (2022). Assessing the potential for crop albedo enhancement in reducing heatwave frequency, duration, and intensity under future climate change. Weather and Climate Extremes, 35, 100415. https://doi.org/10.1016/j.wace.2022.100415
- Knist, S., Goergen, K., Buonomo, E., Christensen, O. B., Colette, A., Cardoso, R. M., et al. (2017). Land-atmosphere coupling in EURO-CORDEX evaluation experiments. *Journal of Geophysical Research: Atmospheres*, 122(1), 79–103. https://doi.org/10.1002/2016jd025476
- Krakauer, N. Y., Cook, B. I., & Puma, M. J. (2020). Effect of irrigation on humid heat extremes. Environmental Research Letters, 15(9), 094010. https://doi.org/10.1088/1748-9326/ab9ecf
- Lewis, S. C., & King, A. D. (2015). Dramatically increased rate of observed hot record breaking in recent Australian temperatures. *Geophysical Research Letters*, 42(18), 7776–7784. https://doi.org/10.1002/2015gl065793
- Lorenz, R., Argüeso, D., Donat, M. G., Pitman, A. J., van den Hurk, B., Berg, A., et al. (2016). Influence of land-atmosphere feedbacks on temperature and precipitation extremes in the GLACE-CMIP5 ensemble. *Journal of Geophysical Research: Atmospheres*, 121(2), 607–623. https://doi.org/10.1002/2015jd024053
- Lorenz, R., Jaeger, E. B., & Seneviratne, S. I. (2010). Persistence of heat waves and its link to soil moisture memory. Geophysical Research Letters, 37(9), L09703. https://doi.org/10.1029/2010gl042764
- Lurton, T., Balkanski, Y., Bastrikov, V., Bekki, S., Bopp, L., Braconnot, P., et al. (2020). Implementation of the CMIP6 forcing data in the IPSL-CM6A-LR model. *Journal of Advances in Modeling Earth Systems*, 12(4). https://doi.org/10.1029/2019ms001940
- Mauritsen, T., Bader, J., Becker, T., Behrens, J., Bittner, M., Brokopf, R., et al. (2019). Developments in the MPI-M Earth system model version 1.2 (MPI-ESM1.2) and its response to increasing CO₂. Journal of Advances in Modeling Earth Systems, 11(4), 998–1038. https://doi.org/10. 1029/2018ms001400
- McKinnon, K. A., Poppick, A., & Simpson, I. R. (2021). Hot extremes have become drier in the United States Southwest. *Nature Climate Change*, 11(7), 598–604. https://doi.org/10.1038/s41558-021-01076-9
- Miralles, D. G., Gentine, P., Seneviratne, S. I., & Teuling, A. J. (2019). Land-atmospheric feedbacks during droughts and heatwaves: State of the science and current challenges. *Annals of the New York Academy of Sciences*, 1436(1), 19–35. https://doi.org/10.1111/nyas.13912
- Miralles, D. G., Teuling, A. J., van Heerwaarden, C. C., & Vilà-Guerau de Arellano, J. (2014). Mega-heatwave temperatures due to combined soil desiccation and atmospheric heat accumulation. *Nature Geoscience*, 7(5), 345–349. https://doi.org/10.1038/ngeo2141
- Mishra, V., Mukherjee, S., Kumar, R., & Stone, D. A. (2017). Heat wave exposure in India in current, 1.5°C, and 2.0°C worlds. Environmental Research Letters, 12(12), 124012. https://doi.org/10.1088/1748-9326/aa9388
- Mora, C., Dousset, B., Caldwell, I. R., Powell, F. E., Geronimo, R. C., Bielecki, C. R., et al. (2017). Global risk of deadly heat. *Nature Climate Change*, 7(7), 501–506. https://doi.org/10.1038/nclimate3322
- Mueller, B., & Seneviratne, S. I. (2012). Hot days induced by precipitation deficits at the global scale. Proceedings of the National Academy of Sciences of the United States of America, 109(31), 12398–12403. https://doi.org/10.1073/pnas.1204330109
- Nairn, J., Ostendorf, B., & Bi, P. (2018). Performance of excess heat factor severity as a global heatwave health impact index. *International Journal of Environmental Research and Public Health*, 15(11), 2494. https://doi.org/10.3390/ijerph15112494
- Nairn, J. R., & Fawcett, R. J. (2014). The excess heat factor: A metric for heatwave intensity and its use in classifying heatwave severity. International Journal of Environmental Research and Public Health, 12(1), 227–253. https://doi.org/10.3390/ijerph120100227
- O'Neill, B. C., Tebaldi, C., van Vuuren, D. P., Eyring, V., Friedlingstein, P., Hurtt, G., et al. (2016). The scenario model intercomparison project (ScenarioMIP) for CMIP6. Geoscientific Model Development, 9(9), 3461–3482. https://doi.org/10.5194/gmd-9-3461-2016
- Onuma, Y., & Kim, H. (2021). MIROC MIROC6 model output prepared for CMIP6 LS3MIP amip-lfmip-pdLC [Dataset]. https://doi.org/10.22033/ESGF/CMIP6.5440
- Perkins, S. E. (2015). A review on the scientific understanding of heatwaves—Their measurement, driving mechanisms, and changes at the global scale. Atmospheric Research, 164–165, 242–267, https://doi.org/10.1016/j.atmosres.2015.05.014
- Perkins, S. E., & Alexander, L. V. (2013). On the measurement of heat waves. *Journal of Climate*, 26(13), 4500–4517. https://doi.org/10.1175/jcli-d-12-00383.1
- Perkins, S. E., Alexander, L. V., & Nairn, J. R. (2012). Increasing frequency, intensity and duration of observed global heatwaves and warm spells. Geophysical Research Letters, 39(20), L20714. https://doi.org/10.1029/2012gl053361
- Perkins, S. E., Argüeso, D., & White, C. J. (2015). Relationships between climate variability, soil moisture, and Australian heatwaves. *Journal of Geophysical Research: Atmospheres*, 120(16), 8144–8164. https://doi.org/10.1002/2015jd023592
- Perkins-Kirkpatrick, S. E., & Lewis, S. C. (2020). Increasing trends in regional heatwaves. *Nature Communications*, 11(1), 3357. https://doi.org/10.1038/s41467-020-16970-7
- Pitman, A. J., Avila, F. B., Abramowitz, G., Wang, Y. P., Phipps, S. J., & de Noblet-Ducoudré, N. (2011). Importance of background climate in determining impact of land-cover change on regional climate. *Nature Climate Change*, 1(9), 472–475. https://doi.org/10.1038/nclimate1294
- Portmann, R., Beyerle, U., Davin, E., Fischer, E. M., De Hertog, S., & Schemm, S. (2022). Global forestation and deforestation affect remote climate via adjusted atmosphere and ocean circulation. *Nature Communications*, 13(1), 5569. https://doi.org/10.1038/s41467-022-33279-9
- Qiao, L., Zuo, Z., Zhang, R., Piao, S., Xiao, D., & Zhang, K. (2023). Soil moisture-atmosphere coupling accelerates global warming. *Nature Communications*, 14(1), 4908. https://doi.org/10.1038/s41467-023-40641-y
- Rogers, C. D. W., Ting, M., Li, C., Kornhuber, K., Coffel, E. D., Horton, R. M., et al. (2021). Recent increases in exposure to extreme humid-heat events disproportionately affect populated regions. *Geophysical Research Letters*, 48(19), e2021GL094183. https://doi.org/10.1029/2021gl094183
- Schulzweida, U. (2023). CDO user guide (version 2.3.0). Zenodo. https://doi.org/10.5281/zenodo.10020800
- Seneviratne, S. I., Corti, T., Davin, E. L., Hirschi, M., Jaeger, E. B., Lehner, I., et al. (2010). Investigating soil moisture–climate interactions in a changing climate: A review. *Earth-Science Reviews*, 99(3–4), 125–161. https://doi.org/10.1016/j.earscirev.2010.02.004
- Seneviratne, S. I., Luthi, D., Litschi, M., & Schar, C. (2006). Land-atmosphere coupling and climate change in Europe. *Nature*, 443(7108), 205–209. https://doi.org/10.1038/nature05095

ZHOU ET AL. 12 of 13

23284277, 2024, 7, Down

- Seneviratne, S. I., Phipps, S. J., Pitman, A. J., Hirsch, A. L., Davin, E. L., Donat, M. G., et al. (2018). Land radiative management as contributor to regional-scale climate adaptation and mitigation. *Nature Geoscience*, 11(2), 88–96. https://doi.org/10.1038/s41561-017-0057-5
- Seneviratne, S. I., Wilhelm, M., Stanelle, T., Hurk, B., Hagemann, S., Berg, A., et al. (2013). Impact of soil moisture-climate feedbacks on CMIP5 projections: First results from the GLACE-CMIP5 experiment. *Geophysical Research Letters*, 40(19), 5212–5217. https://doi.org/10.1002/grl. 50956
- Seneviratne, S. I., Zhang, X., Adnan, M., Badi, W., Dereczynski, C., Di Luca, A., et al. (2021). Weather and climate extreme events in a changing climate. In V. Masson-Delmotte, P. Zhai, A. Pirani, S. L. Connors, C. Péan, S. Berger, et al. (Eds.), Climate change 2021: The physical science basis. Contribution of working group I to the sixth assessment report of the intergovernmental panel on climate change (pp. 1513–1766). Cambridge University Press.
- Shiogama, H., Abe, M., & Tatebe, H. (2019a). MIROC6 model output prepared for CMIP6 ScenarioMIP ssp585 [Dataset]. https://doi.org/10.22033/ESGF/CMIP6.5771
- Shiogama, H., Abe, M., & Tatebe, H. (2019b). MIROC MIROC6 model output prepared for CMIP6 ScenarioMIP ssp126 [Dataset]. https://doi.org/10.22033/ESGF/CMIP6.5743
- Stacke, T., Wieners, K.-H., Giorgetta, M., Jungclaus, J., Reick, C., Esch, M., et al. (2019). MPI-M MPI-ESM1.2-LR model output prepared for CMIP6 LS3MIP amip-lfmip-pdLC [Dataset]. https://doi.org/10.22033/ESGF/CMIP6.6474
- State of the Climate: Global Climate Report for Annual 2020. (2020a). State of the Climate: Global Climate Report for Annual 2020. Retrieved from https://www.ncdc.noaa.gov/sotc/global/202013
- State of the Climate: Global Climate Report for August 2020. (2020b). State of the Climate: Global Climate Report for August 2020. Retrieved from https://www.ncdc.noaa.gov/sotc/global/202008
- Tatebe, H., Ogura, T., Nitta, T., Komuro, Y., Ogochi, K., Takemura, T., et al. (2019). Description and basic evaluation of simulated mean state, internal variability, and climate sensitivity in MIROC6. *Geoscientific Model Development*, 12(7), 2727–2765. https://doi.org/10.5194/gmd-12-2727-2010
- Tatebe, H., & Watanabe, M. (2018). MIROC MIROC6 model output prepared for CMIP6 CMIP historical [Dataset]. https://doi.org/10.22033/ ESGE/CMIP6 5603
- Tebaldi, C., Debeire, K., Eyring, V., Fischer, E., Fyfe, J., Friedlingstein, P., et al. (2021). Climate model projections from the scenario model intercomparison project (ScenarioMIP) of CMIP6. Earth System Dynamics. 12(1), 253–293, https://doi.org/10.5194/esd-12-253-2021
- Teuling, A. J., Seneviratne, S. I., Stöckli, R., Reichstein, M., Moors, E., Ciais, P., et al. (2010). Contrasting response of European forest and grassland energy exchange to heatwaves. *Nature Geoscience*, 3(10), 722–727. https://doi.org/10.1038/ngeo950
- Thiery, W., Visser, A. J., Fischer, E. M., Hauser, M., Hirsch, A. L., Lawrence, D. M., et al. (2020). Warming of hot extremes alleviated by expanding irrigation. *Nature Communications*, 11(1), 290. https://doi.org/10.1038/s41467-019-14075-4
- Thorne, P. W., Donat, M. G., Dunn, R. J. H., Williams, C. N., Alexander, L. V., Caesar, J., et al. (2016). Reassessing changes in diurnal temperature range: Intercomparison and evaluation of existing global data set estimates. *Journal of Geophysical Research: Atmospheres*, 121(10), 5138–5158. https://doi.org/10.1002/2015jd024584
- Tomasini, M., Guichard, F., Couvreux, F., Roehrig, R., & Barbier, J. (2022). Spurious effects of the deep convection parameterisation on the simulation of a Sahelian heatwave. *Quarterly Journal of the Royal Meteorological Society*, 148(748), 3071–3098. https://doi.org/10.1002/qj.
- van den Hurk, B., Kim, H., Krinner, G., Seneviratne, S. I., Derksen, C., Oki, T., et al. (2016). LS3MIP (v1.0) contribution to CMIP6: The land surface, snow and soil moisture model intercomparison project—Aims, setup and expected outcome. *Geoscientific Model Development*, 9(8), 2809–2832. https://doi.org/10.5194/gmd-9-2809-2016
- Vogel, M. M., Orth, R., Cheruy, F., Hagemann, S., Lorenz, R., van den Hurk, B. J. J. M., & Seneviratne, S. I. (2017). Regional amplification of projected changes in extreme temperatures strongly controlled by soil moisture-temperature feedbacks. *Geophysical Research Letters*, 44(3), 1511–1519. https://doi.org/10.1002/2016gl071235
- Vogel, M. M., Zscheischler, J., Fischer, E. M., & Seneviratne, S. I. (2020). Development of future heatwaves for different hazard thresholds. Journal of Geophysical Research: Atmospheres, 125(9), e2019JD032070. https://doi.org/10.1029/2019jd032070
- Vogel, M. M., Zscheischler, J., & Seneviratne, S. I. (2018). Varying soil moisture–atmosphere feedbacks explain divergent temperature extremes and precipitation projections in central Europe. Earth System Dynamics, 9(3), 1107–1125. https://doi.org/10.5194/esd-9-1107-2018
- Wang, J., Chen, Y., Liao, W., He, G., Tett, S. F. B., Yan, Z., et al. (2021). Anthropogenic emissions and urbanization increase risk of compound hot extremes in cities. *Nature Climate Change*, 11(12), 1084–1089. https://doi.org/10.1038/s41558-021-01196-2
- Wieners, K.-H., Giorgetta, M., Jungclaus, J., Reick, C., Esch, M., Bittner, M., et al. (2019a). MPI-M MPI-ESM1.2-LR model output prepared for CMIP6 ScenarioMIP ssp126 [Dataset]. https://doi.org/10.22033/ESGF/CMIP6.6690
- Wieners, K.-H., Giorgetta, M., Jungclaus, J., Reick, C., Esch, M., Bittner, M., et al. (2019b). MPI-M MPI-ESM1.2-LR model output prepared for CMIP6 ScenarioMIP ssp585 [Dataset]. https://doi.org/10.22033/ESGF/CMIP6.6705
- Wieners, K.-H., Giorgetta, M., Jungclaus, J., Reick, C., Esch, M., Bittner, M., et al. (2019c). MPI-M MPI-ESM1.2-LR model output prepared for CMIP6 CMIP historical [Dataset]. https://doi.org/10.22033/ESGF/CMIP6.6595
- Wouters, H., Keune, J., Pertrova, I. Y., van Heerwaarden, C. C., Teuling, A. J., Pal, J. S., et al. (2022). Soil drought can mitigate deadly heat stress thanks to a reduction of air humidity. *Science Advances*, 8(1). https://doi.org/10.1126/sciadv.abe6653
- Xu, Z., FitzGerald, G., Guo, Y., Jalaludin, B., & Tong, S. (2016). Impact of heatwave on mortality under different heatwave definitions: A systematic review and meta-analysis. *Environment International*, 89–90, 193–203. https://doi.org/10.1016/j.envint.2016.02.007
- Yang, J., Zhou, M., Ren, Z., Li, M., Wang, B., Liu, L., et al. (2021). Projecting heat-related excess mortality under climate change scenarios in China. *Nature Communications*, 12(1), 1039. https://doi.org/10.1038/s41467-021-21305-1
- Zachariah, M., T, A., AchutaRao, K. M., Saeed, F., Jha, R., Dhasmana, M. K., et al. (2023). Attribution of 2022 early-spring heatwave in India and Pakistan to climate change: Lessons in assessing vulnerability and preparedness in reducing impacts. *Environmental Research: Climate*, 2(4), 045005. https://doi.org/10.1088/2752-5295/acf4b6
- Zhang, J., Wu, L., & Dong, W. (2011). Land-atmosphere coupling and summer climate variability over East Asia. *Journal of Geophysical Research*, 116(D5), D05117. https://doi.org/10.1029/2010jd014714
- Zheng, Z., Zhao, L., & Oleson, K. W. (2021). Large model structural uncertainty in global projections of urban heat waves. Nature Communications, 12(1), 3736. https://doi.org/10.1038/s41467-021-24113-9
- Zhou, J., Teuling, A. J., Seneviratne, S., & Hirsch, A. L. (2024). Related codes and data used in soil moisture-temperature coupling increases population exposure to future heatwaves [Dataset and Codes]. https://doi.org/10.5281/zenodo.11004427
- Zhou, S., & Yuan, X. (2022). Upwind droughts enhance half of the heatwaves over North China. Geophysical Research Letters, 49(2), e2021GL096639. https://doi.org/10.1029/2021gl096639

ZHOU ET AL. 13 of 13